PCCP

COMMUNICATION

View Article Online
View Journal | View Issue

Open Access Article. Published on 24 July 2014. Downloaded on 3/30/2026 1:22:35 AM.
This article is licensed under a Creative Commons Attribution 3.0 Unported Licence.

Cite this: *Phys. Chem. Chem. Phys.*, 2014, **16**, 18690

Received 22nd May 2014,
Accepted 22nd July 2014

DOI: 10.1039/c4cp02238f

www.rsc.org/pccp

Fabrication of silver nanoparticles with limited size distribution on TiO_2 containing zeolites†

Andrea Mazzocut,[a] Eduardo Coutino-Gonzalez,[b] Wouter Baekelant,[b] Bert Sels,[c] Johan Hofkens[ab] and Tom Vosch*[a]

Here we present a simple route to produce well-defined photo-reduced silver nanoparticles on TiO_2 containing zeolites. We used natural and artificial irradiation sources to study their effect on the particle size distribution. The samples were investigated by electron microscopy, X-ray diffraction, fluorescence microscopy and UV-Vis diffuse reflectance spectroscopy.

The photo-catalytic properties of titanium dioxide (TiO_2) were demonstrated in the early 70's by Fujishima and Honda, who showed the O_2 evolution from a TiO_2 electrode in water solution upon irradiation with UV light.[1] The process relies on a photon-mediated promotion of an electron from the valence band (VB) to the conduction band (CB) of the semiconductor, leaving an electron vacancy, known as a hole, in the VB. The formed electrons and holes can then either recombine or be involved in redox reactions at the interface.[2] Advantages of titanium dioxide with respect to other semiconductors are the high tolerance to light-induced corrosion,[3] the abundant presence on Earth and its low cost. Such characteristics made TiO_2 the candidate of choice in a wide range of applications such as catalysts for water-splitting[4,5] water purification[6] and as materials in certain solar cell applications.[7,8] This study combines the photo-catalytic properties of TiO_2 with the structural properties of silver-exchanged zeolites,[9,10] to fabricate uniform-sized dispersed silver nanoparticles on zeolites that could potentially be used for applications like surface enhanced Raman spectroscopy (SERS)[11,12] or as catalytic bodies.[13] In previous reports, the use of silver zeolite composites for Raman enhancement showed a great improvement in signal thanks to the presence of metals on the zeolites surface.[11] Since then, several synthesis procedures have emerged to fabricate these types of materials. For instance, Dutta and Robins[14] used a reducing agent and a subsequent heat treatment to obtain, starting from silver-exchanged zeolites, a large distribution of spheres with sizes ranging from 10 nm to 1 μm. A different route was reported by Yan and collaborators[15] who used a vacuum deposition method to form a thin layer of metallic silver on the zeolite crystal surfaces. For applications in SERS and catalysis, materials with a uniform distributed particle size on the surface are the most interesting. Therefore we studied different zeolite frameworks (FAU and LTA) to find the optimal conditions to produce well-defined silver nanoparticles on titanium dioxide containing zeolites. We present here a simple route to fabricate silver nanoparticles with limited size distribution from Ag-exchanged zeolites by using the photo-catalytic properties of TiO_2.

Hydrated 3A, 4A, 5A (LTA) and Y (FAU) zeolites were provided by UOP (see Fig. S1, ESI†). Silver nitrate ($AgNO_3$, 99% Sigma Aldrich) and titanium isopropoxide (97% Sigma Aldrich) were also used. A cation exchange procedure was employed to synthesize the silver exchanged zeolites.[16] One gram of the zeolite material was suspended in 500 mL of an aqueous silver nitrate solution (0.8–1.5 mM, the concentration was adjusted to obtain 8% of Ag weight in the samples), then the sample was stirred for 2 hours in the dark. The sample was recovered by filtration using a Buchner filter and washed several times with miliQ water, the recovered powder was dried at 373 K for 1 hour. The water content in the zeolite was calculated by weighing a small amount of zeolite (1 g) before and after heat treatment at 723 K for 5 h, the results showed an average of 20% w/w of water trapped in the zeolite materials. The trapped water content information is needed to correctly determine the amount of exchanged silver ions. Samples were named starting with the framework type (3A, 4A, 5A and Y) followed by the weight percentage of the silver content as follows 3A_8Ag, 4A_8Ag, 5A_8Ag and Y_8Ag, respectively. To incorporate TiO_2 into the zeolites we followed the procedure previously described by Dubey and collaborators,[17] which involves a physical mix of the TiO_2 precursor (titanium isopropoxide) with the silver

[a] *Nano-Science Center, Department of Chemistry, University of Copenhagen, Universitetsparken 5, 2100 Copenhagen, Denmark. E-mail: tom@chem.ku.dk; Fax: +45-353-20322; Tel: +45-353-20313*
[b] *Department of Chemistry, KU Leuven, Celestijnenlaan 200F, B-3001 Leuven, Belgium*
[c] *Department of Microbial and Molecular Systems, Centre for Surface Chemistry and Catalysis, KU Leuven, Kasteelpark Arenberg 23, B-3001 Leuven, Belgium*

† Electronic supplementary information (ESI) available: SEM & TEM images, DRS spectra, description of the fluorescence microscope set-up, additional XRD patterns. See DOI: 10.1039/c4cp02238f

This journal is © the Owner Societies 2014

Open Access Article. Published on 24 July 2014. Downloaded on 3/30/2026 1:22:35 AM.
This article is licensed under a Creative Commons Attribution 3.0 Unported Licence.

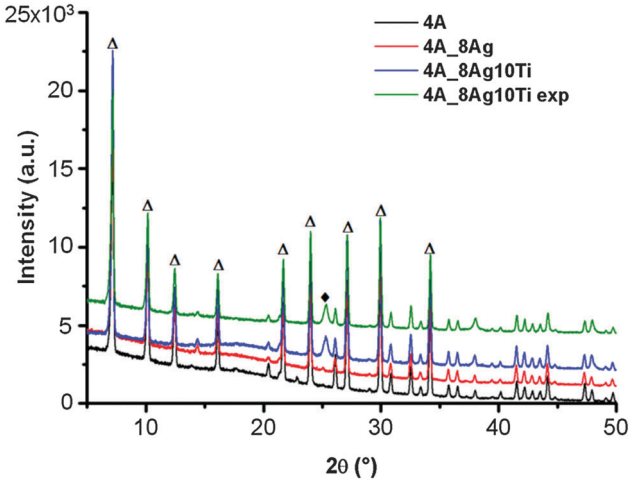

Fig. 1 Diffraction pattern of the parent, silver exchanged and Ti incorporated 4A zeolite before and after UV exposure. Typical zeolite LTA patterns are indicated with △, whereas ◆ was used to indicate the positions of the reflection peaks due to TiO_2 in its anatase phase.

exchanged zeolite and a calcination step at 723 K. By following this procedure, TiO_2 is expected to be attached to the outer part of the zeolite crystals.[17,18] For all samples a 10% w/w of TiO_2 was used since previous research showed that an increase in the titanium loading affected the zeolite crystallinity.[19] The samples were calcined, for 5 h at 723 K following 2 steps of 15 minutes each at 373 and 433 K to prevent any damage in the zeolite structure. The samples were named by adding the TiO_2 content to the previous silver exchanged zeolite (3A_8Ag10Ti, 4A_8Ag10Ti, 5A_8Ag10Ti and Y_8Ag_10Ti).

An XRD analysis was performed to investigate the crystallinity of the samples and the degree of functionalization. As references, a spectrum obtained from the Database of Zeolite Structures[20] and the parent commercial zeolites were used (Fig. S3, ESI†). A comparison between the different starting materials (Fig. 1) confirmed the purity and crystallinity of the different zeolites used in this study. Impregnation of the zeolite crystals with TiO_2 did not affect the zeolite crystal structure, as no observable shift or widening of the characteristic zeolite reflections was observed. A characteristic reflection at $2\theta = 25.3^\circ$ in the TiO_2 containing Ag-zeolites indicates the presence of TiO_2 in the anatase phase (JPCDS 21-1272), which has been reported to be the most photoactive species.[21–23] The other characteristic peaks of the anatase phase are not visible due to its small amount and the overlap with the zeolite reflections. To investigate the possible destruction of the zeolite crystal structure upon photo-reduction, an XRD analysis of the exposed 4A_8Ag10Ti sample was performed (4A_8Ag10Tiexp; top spectrum in Fig. 1). The reduction of silver did not significantly affect the crystallinity of the samples and no difference in reflection patterns was found compared to the non-exposed samples. The same behaviour was observed in the other zeolites (see Fig. S4–S6 in the ESI†).

Heat-treated silver-exchanged zeolites possess peculiar luminescent properties[24] arising from Ag-clusters[25] confined in zeolite cavities. Fig. S7 (ESI†) shows an example of the typical

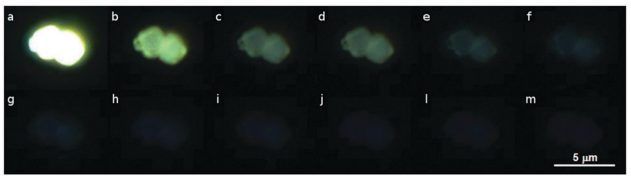

Fig. 2 True color fluorescence microscopy images of day light-exposed 4A_8Ag10Ti upon UV excitation. Time interval between images, 10 seconds. A fast photobleaching of the luminescence in 4A_8Ag10Ti upon UV excitation was observed.

UV-photo-activation process leading to a 20-fold increase in the fluorescence signal of a nonheat-treated 3A_8Ag.[26] The photo-reduction conducted on the Ag/Ti zeolites used in this study, could affect the nature of such luminescent clusters, resulting in a change of their optical properties. Therefore, we investigated the luminescence of individual crystallites using a wide-field fluorescence microscope (see S4, ESI† for experimental details). Upon UV exposure a fast photo-bleaching in heat-treated Ag/Ti containing zeolites was observed (see Fig. 2 for an example of 4A_8Ag10Ti and Fig. S7 in the ESI† for a similar example of 3A_8Ag10Ti). Similar results were also found at the bulk scale, monitoring the emission change in the fluorimeter (see Fig. S8, ESI†). Photo-bleaching was accompanied by a change in the powder color, from an initial white to a dark gray color, indicating the formation of reduced silver nanoparticles. To prove the presence of silver nanoparticles on the zeolite crystals surfaces, transmission electron microscopy (TEM) and scanning electron microscopy (SEM) were employed. The samples were suspended in miliQ water (1 mg mL^{-1}), exposed to daylight for 2 days and then deposited on a copper TEM grid. Fig. 3 shows the image and particle size distribution of daylight exposed 4A_8Ag10Ti. The presence of silver nanoparticles on the zeolite surfaces is clearly evident in all samples (see also Fig. S10, ESI†).

In LTA zeolites, the average Ag particle diameter was found to be between 4 and 7 nm (see Fig. 3 and Fig. S10, ESI†), whereas a wider range of size distributions spanning from 5 to 14 nm, was observed in the Y_8Ag10Ti sample, with an average diameter around 9.5 nm (Fig. S10, ESI†). The presence of larger nanoparticles (>20 nm) was also observed, albeit in minor proportion. Longer exposure times (up to 2 weeks) did not lead to significant differences in silver nanoparticles size distribution. The particle dimensions on the surface of zeolites are larger than the openings and cavities found in the zeolite material

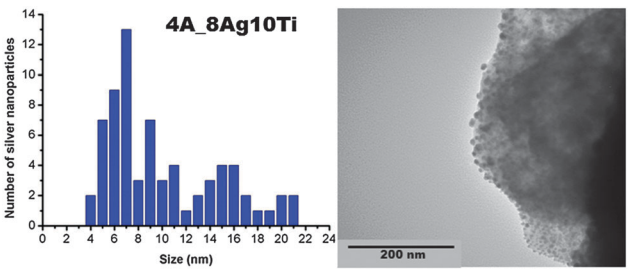

Fig. 3 Left, particle size distribution and right, the TEM micrograph of the daylight exposed 4A_8Ag_10Ti.

Open Access Article. Published on 24 July 2014. Downloaded on 3/30/2026 1:22:35 AM.
This article is licensed under a Creative Commons Attribution 3.0 Unported Licence.

(Table S2, ESI†), indicating that smaller silver species diffuse through the openings to form large nanoparticles on the surface. The nature of the nanostructures observed on the surface of Ag/Ti containing zeolites was investigated by energy-dispersive X-ray (EDX) analysis (Fig. S14, ESI†). The obtained spectrum showed a high silver peak resulting from the photo-reduction of the samples. Further confirmation was obtained when two Ag-free samples with 10% titanium dioxide exposed to daylight were analyzed. These samples showed clean surfaces with a complete absence of particles (Fig. S13, ESI†).

To investigate a possible relationship between the particle size distribution and the UV irradiation source, different samples were prepared using daylight, a handheld UV lamp and a UV photoreactor (366 nm, 1 mW cm^{-2}, see S2, ESI†). These different samples were analysed by TEM and SEM. TEM was used to compare the size distribution of the silver particles using daylight exposed samples and samples that were exposed for 15 minutes using a handheld lamp (after exposure they were stored in the dark until mounted into the TEM). The UV handheld lamp irradiation affected both, the size distribution and the morphology of the photo-reduced silver nanoparticles and revealed larger particle diameters and more irregular (non-spherical) shapes compared to the daylight exposed samples (Fig. S11 and S12, ESI†). The latter could be due to the higher UV flux in the handheld UV lamp, compared to daylight. SEM was used to compare a non-UV illuminated 4A_8Ag10Ti sample and a sample that was exposed to UV irradiation for 15 minutes in a photoreactor. Fig. 4 shows a uniform spatial distribution of silver nanoparticles on the surface of Ag/Ti containing zeolites for the UV exposed samples, whereas no such particles were observed for the non-illuminated sample. The latter clearly indicates that the silver nanoparticle formation on the surface is light induced.

Finally, we recorded diffuse reflectance spectra (DRS) of the materials used in the UV-Vis range during the different stages of sample preparation (Fig. 5). Only weak signals in the DRS spectra of non-exchanged zeolites were found below 300 nm, which is in good agreement with previous reports.[27] The silver loaded zeolites showed stronger signals in the UV region (200–300 nm). Such signals have been previously attributed to isolated silver ions located at specific sites within the zeolite framework in silver exchanged LTA and FAU zeolites.[27,28] Next, we recorded

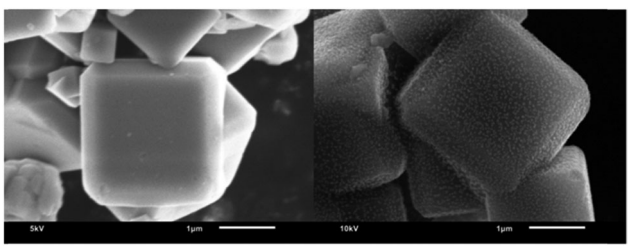

Fig. 4 SEM images of non-illuminated (left) 4A_8Ag10Ti and (right) UV irradiated (15 minutes) 4A_8Ag10Ti. A very uniform spatial distribution of silver nanoparticles is observed on the surface of the UV irradiated 4A_8Ag10Ti zeolite crystals, whereas clean surfaces were found in non-illuminated 4A_8Ag10Ti zeolite crystals (see Fig. S9, ESI† for a larger version of this figure).

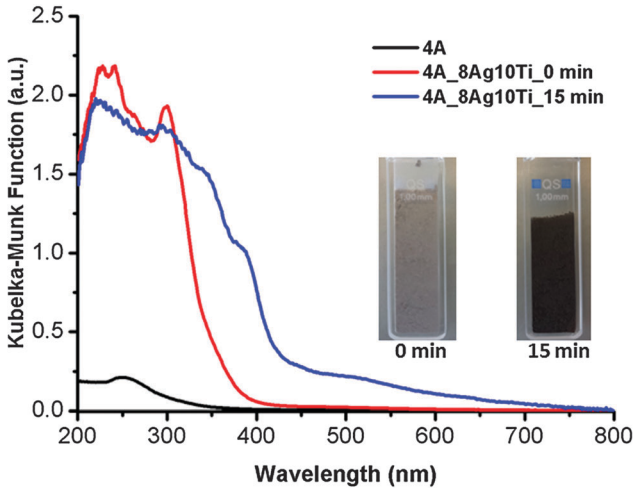

Fig. 5 Kubelka–Munk spectra of the parent zeolite (4A), as-prepared 4A_8Ag10Ti and UV irradiated 4A_8Ag10Ti after 15 minutes of exposure. Inset: photographs of 4A_8Ag10Ti before and after UV irradiation.

DRS spectra of the Ag/Ti containing zeolites (4A_8Ag10Ti) at different irradiation times. At zero irradiation time the typical absorption band of TiO_2 was observed (Fig. 5), which is located in the UV region (200–340 nm) and covered the signals of different silver species (ions, clusters) encountered in Ag-zeolites. After 15 minutes of UV exposure in the photoreactor, the appearance of pronounced bands at 360 and 390 nm (Fig. 5) was observed. The new features are likely due to surface plasmon resonance (SPR) of silver nanoparticles. Similar plasmon bands have been previously observed in Ti-mesoporous silica composites containing silver nanoparticles with sizes ranging from 4.7 to 7.6 nm.[29]

To summarize, we demonstrated a simple way to photo-convert Ag species, trapped in the zeolite cages of silver exchanged zeolites, into well-dispersed metallic silver nanoparticles with sizes ranging from 4 to 8 nm on the surfaces of TiO_2 impregnated zeolite crystals. The particles (as seen by SEM and TEM) were confirmed by EDX analysis to be silver nanoparticles and the presence of their related plasmon bands was indicated by UV-Vis DRS. The versatility of Ag/Ti containing zeolite composites to be incorporated into different substrates and the limited size distribution of the silver nanoparticles make such materials of great interest for potential applications like in SERS and catalysis. A comparison between naturally (daylight) and artificially (UV lamp and UV photoreactor) irradiated samples revealed a difference in particle size dispersion of the photo-reduced silver nanoparticles. Larger and less defined silver nanoparticles were observed in artificially irradiated samples.

Acknowledgements

T.V. gratefully acknowledges financial support from ''Center for Synthetic Biology'' at Copenhagen University funded by the UNIK research initiative of the Danish Ministry of Science, Technology and Innovation (Grant 09-065274). We like to thank UOP Antwerpen for their donation of the 3A, 4A, 5A (LTA) and Y (FAU) zeolites.

This journal is © the Owner Societies 2014

Open Access Article. Published on 24 July 2014. Downloaded on 3/30/2026 1:22:35 AM.
This article is licensed under a Creative Commons Attribution 3.0 Unported Licence.

Notes and references

1 A. Fujishima and K. Honda, *Nature*, 1972, **238**, 37–38.
2 U. I. Gaya and A. H. Abdullah, *J. Photochem. Photobiol., C*, 2008, **9**, 1–12.
3 J. Nowotny, T. Bak, M. K. Nowotny and L. R. Sheppard, *Int. J. Hydrogen Energy*, 2007, **32**, 2609–2629.
4 M. Ni, M. K. H. Leung, D. Y. Leung and K. Sumathy, *Renewable Sustainable Energy Rev.*, 2007, **11**, 401–425.
5 V. J. Babu, M. K. Kumar, A. S. Nair, T. L. Kheng, S. I. Allakhverdiev and S. Ramakrishna, *Int. J. Hydrogen Energy*, 2012, 1–8.
6 L. Zhang, T. Kanki, N. Sano and A. Toyoda, *Sep. Purif. Technol.*, 2003, **31**, 105–110.
7 S. Günes, H. Neugebauer, N. S. Sariciftci, J. Roither, M. Kovalenko, G. Pillwein and W. Heiss, *Adv. Funct. Mater.*, 2006, **16**, 1095–1099.
8 A. K. Jana, *J. Photochem. Photobiol., A*, 2000, **132**, 1–17.
9 T. Sun and K. Seff, *Chem. Rev.*, 1994, **94**, 857–870.
10 Y. Yonezawa, N. Kometani, T. Sakaue and A. Yano, *J. Photochem. Photobiol., A*, 2005, **171**, 1–8.
11 W. Yan, L. Bao, S. M. Mahurin and S. Dai, *Appl. Spectrosc.*, 2004, **58**, 18–25.
12 K. G. M. Laurier, M. Poets, F. Vermoortele, G. De Cremer, J. A. Martens, H. Uji-i, D. E. De Vos, J. Hofkens and M. B. J. Roeffaers, *Chem. Commun.*, 2012, **48**, 1559–1601.
13 H. H. Patterson, R. S. Gomez, H. Y. Lu and R. L. Yson, *Catal. Today*, 2007, **120**, 168–173.
14 P. K. Dutta and D. Robins, *Langmuir*, 1991, **7**, 2004–2006.
15 W. Yan, L. Bao and S. M. Mahurin, *Appl. Spectrosc.*, 2004, **58**, 18–25.
16 G. De Cremer, E. Coutino-Gonzalez, M. B. J. Roeffaers, D. E. De Vos, J. Hofkens, T. Vosch and B. F. Sels, *ChemPhysChem*, 2010, **11**, 1627–1631.
17 N. Dubey, N. Labhsetwar and S. Devotta, *Catal. Today*, 2007, **129**, 428–434.
18 M. A. Fox, K. E. Doan and M. T. Dulay, *Res. Chem. Intermed*, 1994, **20**, 711–722.
19 S. M. Kuznicki, K. L. DeVries and E. M. Eyring, *J. Phys. Chem.*, 1980, **84**, 535–537.
20 International Zeolite Association. http://www.iza-online.org.
21 A. Rivera, K. Tanaka and T. Hisanaga, *Appl. Catal., B*, 1993, **3**, 37–44.
22 A. Sclafani and L. Palmisano, *J. Photochem. Photobiol., A*, 1991, **56**, 113–123.
23 Y. Xu and C. H. Langford, *J. Phys. Chem.*, 1995, **99**, 11501–11507.
24 G. De Cremer, E. Coutino-Gonzalez, M. B. J. Roeffaers, B. Moens, J. Ollevier, M. Van der Auweraer, R. Schoonheydt, P. A. Jacobs, F. C. De Schryver and J. Hofkens, *et al.*, *J. Am. Chem. Soc.*, 2009, **131**, 3049–3056.
25 L. Peyser, E. Vinson, P. Bartko and R. M. Dickson, *Science*, 2001, **291**, 103–106.
26 G. De Cremer, Y. Antoku, M. B. J. Roeffaers, M. Sliwa, J. Van Noyen, S. Smout, J. Hofkens, D. E. De Vos, B. F. Sels and T. Vosch, *Angew. Chem., Int. Ed.*, 2008, **120**, 2855–2858.
27 E. Coutino-Gonzalez, D. Grandjean, M. B. J. Roeffaers, K. Kvashnina, E. Fron, B. Dieu, G. De Cremer, P. Lievens, B. F. Sels and J. Hofkens, *Chem. Commun.*, 2014, **50**, 1350–1352.
28 R. Seifert, R. Rytz and G. Calzaferri, *J. Phys. Chem. A*, 2000, **104**, 7473–7483.
29 Y. Horiuchi, M. Shimada, T. Kamegawa, K. Mori and H. Yamashita, *J. Mater. Chem.*, 2009, **19**, 6745–6749.